

<https://doi.org/10.32056/KOMAG2023.1.4>

## The concept of a household low-speed kinetic energy storage

Received: 09.03.2023

Accepted: 25.03.2023

Published online: 03.04.2023

### Author's affiliations and addresses:

<sup>1</sup> KOMAG Institute of Mining Technology, Pszczyńska 37, 44-101 Gliwice, Polska

### \* Correspondence:

e-mail: [sjanas@komag.eu](mailto:sjanas@komag.eu)

**Sebastian JANAS**  <sup>1\*</sup>

### Abstract:

This paper presents a concept of mechanical design, for a slow-speed kinetic energy storage device. It is an attempt to present the problem of using the device to cooperate with small-scale household RES. Calculations allowing for selection of rotating mass along with determination of effective revolutions of the rotating mass are presented. The 3D model gives an overview of the main structural nodes of the device in the mechanical part. Due to large axial load resulting from the mass of the rotor and other components and subassemblies, a simple FEM simulation of the structure base was performed. Preliminary calculations of the magnetic bearing, acting as an axial bearing, were also carried out.

Keywords: kinetic energy storage, household RES, renewable energy, just transition



## 1. Introduction

In the era of diversification of energy production using RES, there is a need to store excess amounts of it. Stabilization of the generated voltage is also an important aspect. RES commonly used in households (in terms of electricity generation) are photovoltaic panels. Household wind farms are less common. However, such systems do not always work properly, especially when the receiving power grid is overloaded while giving electricity to the power system. Also, such systems do not produce electricity in a ready-to-consume form. In such a situation, energy storage facilities collecting the excess electricity for a short time, compensate for temporary voltage spikes, and then, also in a short time, recharge the receiving grid. This energy can be stored in the form of heat or kinetic energy. In the event of a shortage of power from the energy system or renewable energy sources, the stored energy can be used and converted back into electricity.

## 2. Materials review – examples of FESS

There are many solutions for kinetic energy storage used primarily in industry and in RES power plants. These are complex systems with a capacity of at least several hundred kWh. Smaller systems are used in the automotive industry. In Volvo (Fig. 1), the use of a flywheel-based energy storage reduced fuel consumption by up to 25% [1, 2]. The system is installed on the rear axle. During deceleration, braking energy causes the flywheel to spin at 60,000 rpm. When moving off, the rotation of the flywheel is transferred to the rear drive wheels via a special gear. Energy from the wheel can be used to accelerate the vehicle or to move off again. With this solution, the car is best suited to urban driving, where there is a high number of braking and starting cycles.

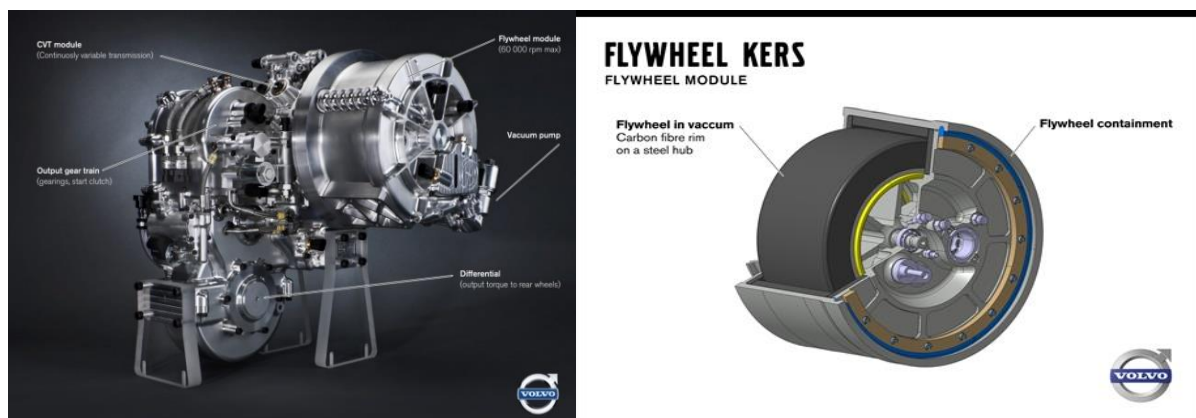


Fig. 1. Example of kinetic energy storage used in a Volvo S60 [1]

Flywheel systems acting as energy storages are used in Electric Multiple Units (EMU) or light-weight locomotives. Energy savings when using a flywheel reach 31%. Operation of such an energy storage is based on receiving braking energy and transferring it to the flywheel. Then, when moving off or driving up a hill, the energy stored in the flywheel is recovered [3]. In heavy long-distance locomotives, such systems did not prove to be useful. This is due to the very large weight of the locomotive, and thus the high energy demand when moving, and the very low frequency of braking. Another example of using FESS can be found on one of the Los Angeles underground lines. The VYCON company installed a train braking energy recovery system at the underground station. Originally, during braking, the energy generated was dissipated via third rail and converted into heat in the braking resistors. Currently, the same energy is converted by an electric machine into kinetic energy of the HSFESS flywheel. When the EMU is moving, the system is switched and the train receives energy through the third rail. In the peak hours of EMU traffic in the underground, the savings reach even 20%. As for Polish solutions, the company MEGATECH TECHNOLOGY Sp. z o.o. on its website informs about the project entitled: "Development of a high-speed PM BLDC motor as a kinetic energy storage device, along with infrastructure ensuring storage recharging and

quick energy recovery and transforming it into a form and parameters that allow for effective use by the standard devices" (POIR.01.02. 00-00-0326/16 of September 29, 2017) [4].

### 3. Results

#### 3.1. Preliminary calculations

Due to the introduction of kinetic energy storage systems in the industrial area, the possibility of using this type of system in households was analyzed. Initially, two cases of FESS were considered. Low Speed Flywheel Energy Storage System (LSFESS) with the rotational speed of the rotating mass up to 10,000 rpm and High Speed Flywheel Energy Storage System (HSFESS) with the speed range from around 10,000 rpm to even more than 100,000 rpm. Design of LSFESS is much simpler, and thus its cost is significantly lower compared to HSFESS. Also, HSFESS units are usually five times more expensive than low-speed energy storages [5, 6].

In order to identify the basic parameters for the selection of the energy storage system, a series of characteristics were defined, which were used to determine the maximum rotational speed of the rotor in relation to its mass and diameter.

The difference in energy of the storage system at the beginning and at the end was used to determine the speed range of the rotating mass:

$$\Delta E = E_1 - E_2 \quad (1)$$

where:

$E_1$  – initial energy of the storage, Ws,

$E_2$  – final energy of the storage, Ws.

After substituting the formula for kinetic energy derived from angular velocities into relationship (1), we obtain:

$$\Delta E = \frac{I \cdot \omega_1^2}{2} - \frac{I \cdot \omega_2^2}{2} \quad (2)$$

where:

$I$  – moment of inertia of a rotating body,  $\text{kg} \cdot \text{m}^2$ ,

$\omega_1$  – initial angular velocity of the rotating body,  $\text{rad} \cdot \text{s}^{-1}$ ,

$\omega_2$  – final angular velocity of the rotating body,  $\text{rad} \cdot \text{s}^{-1}$ .

In order to determine rotational speed at which the rotating mass will accumulate maximum energy, the relationship was determined on the basis of the previously presented formula for kinetic energy and the relationship for the moment of inertia  $I$  of the rotating body:

$$I = \frac{m \cdot R^2}{2} \quad (3)$$

where:

$m$  – mass of a rotating body, kg,

$R$  – radius of a rotating body, m,

and angular velocity of a rotating body:

$$\omega = 2 \cdot \pi \cdot n \quad (4)$$

where:

$n$  – rotational speed of a body,  $\text{rev} \cdot \text{s}^{-1}$ .



After applying the relationships (3) and (4) in the formula for the kinetic energy of the rotating mass, the rotational speed [rev·s<sup>-1</sup>] of the body, at which the rotating mass will accumulate the maximum amount of energy, was determined:

$$n_1 = \sqrt{\frac{E_1}{m \cdot (\pi \cdot R)^2}} \tag{5}$$

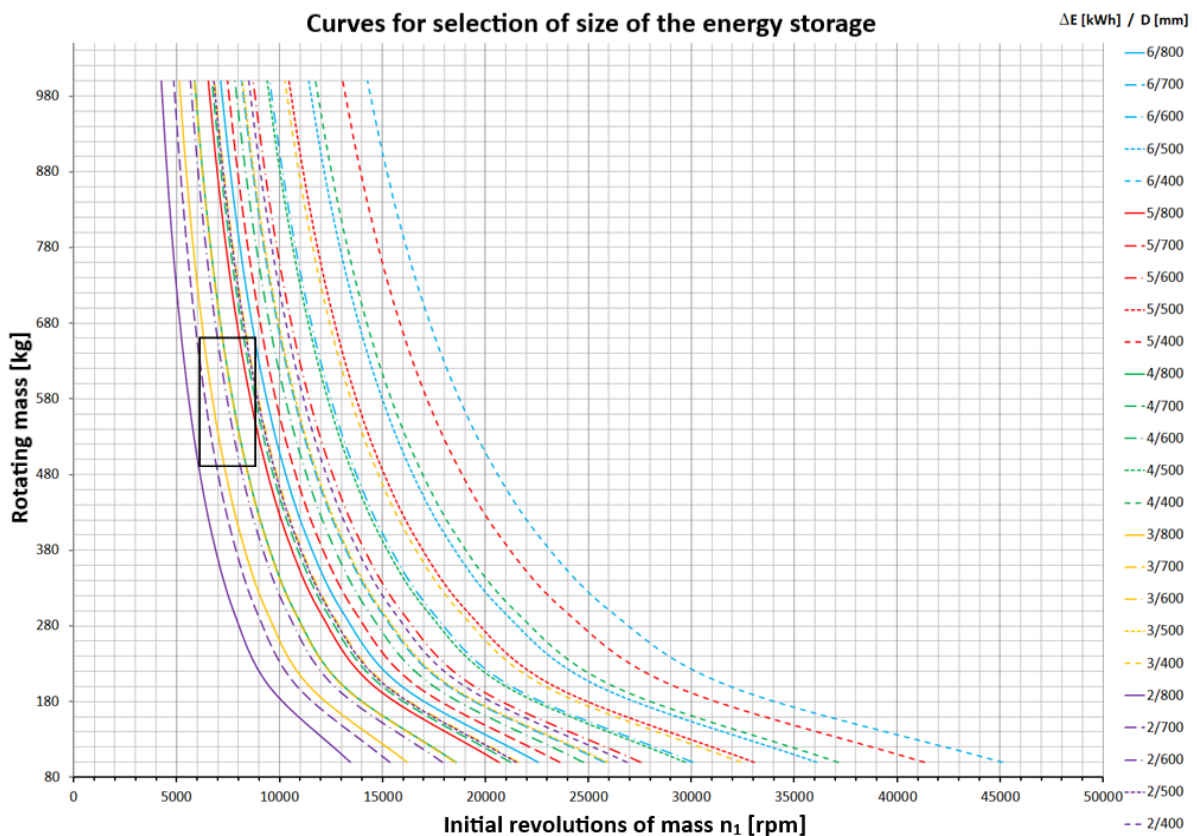
where:

- E<sub>1</sub> – initial (stored) kinetic energy, Ws,
- m – mass of a rotating body, kg,
- R – radius of a rotating body, m.

In order to determine the area in which the optimal input parameters should be sought, the ranges of variables were adopted for the creation of characteristics listed in Table 1.

**Table 1.** Range of variables defining the selection area of basic parameters for energy storage

Parameter	Unit	Value
The amount of energy released, ΔE	kWh	2 ÷ 6
Considered range of masses of a rotating body, m	kg	100 ÷ 1000
Diameter range of a rotating body, R	mm	100 ÷ 800



**Fig. 2.** Selection curves of basic parameters for kinetic energy storage in full range of adopted values

Fig. 2 presents a set of parameters illustrating the mass of storage rotor as a function of rotations for each energy storage capacity and rotating mass diameter. Assuming that the energy storage should

be simple in its form and design and that it is meant to be a low-speed storage and it should store the amount of energy in the range of 2÷6 kWh, the range in which selection of basic parameters will take place was determined. For  $\Delta E = 6$  kWh and minimum revolutions of the mass  $n_2 = 1,550$  rpm, the selection area of the storage parameters was determined, as shown in Fig. 3. Maximum revolutions  $n_1 = 8,650$  rpm, diameter  $D = 800$  mm and rotor mass  $m = 680$  kg were selected for these boundary conditions.

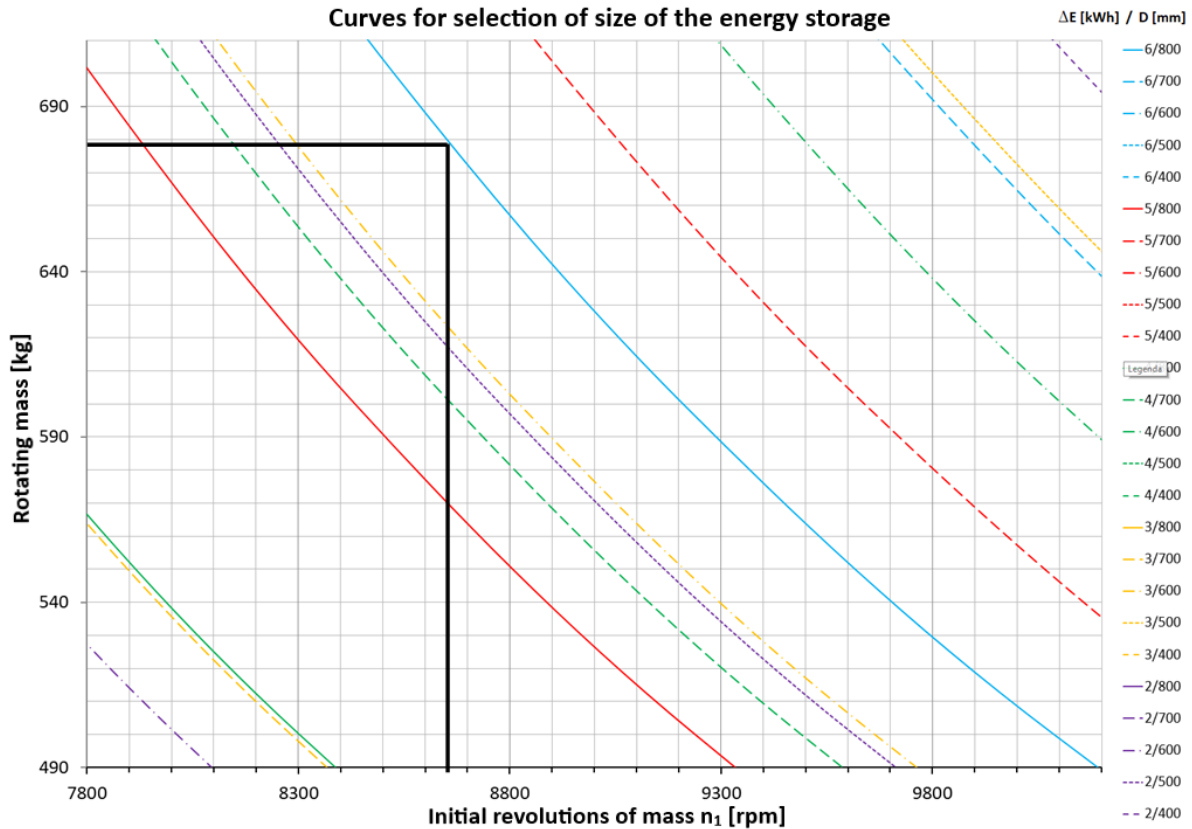
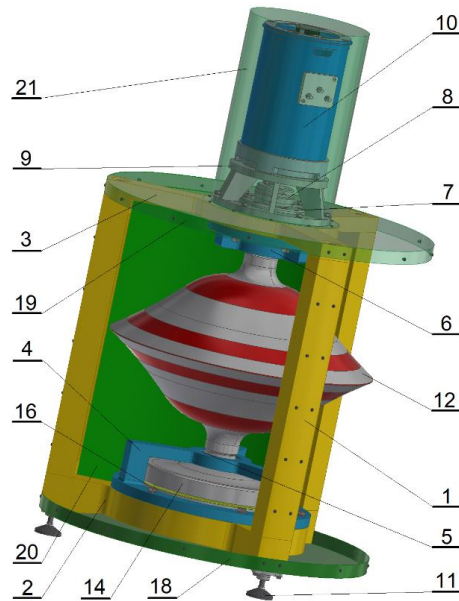


Fig. 3. Curves chosen for selection of basic parameters of kinetic energy storage in the range covering the adopted assumptions

### 3.2. Concept description

Proposed structure is fully assembled from parts and subassemblies. The largest and heaviest component of the device is the rotating mass, which was increased to 890 kg as a result of verification calculations.

The base of the device (Fig. 4) is made of a bolted frame consisting of three pillars (1), which connect the base (2) and the keystone (3). Body (4) of the lower aligning bearing (5) is screwed to the upper surface of the base (2). Body of the upper aligning bearing (6) is screwed to the bottom surface of the keystone (3).



**Fig. 4.** 3D model of kinetic energy storage concept

The mounting flange (7) of the electromagnetic clutch (8) and the bracket (9) of the electric machine (10) are screwed to the upper plane of the keystone. Support feet (11) are installed in the bottom part of the base (2). In the alignment bearings (5 and 6) a rotating mass (12), connected to the electromagnetic clutch (8) by a sleeve, is installed. A disc (14) with a set of permanent magnets is screwed to the lower pivot of the rotating mass. A disc (16) with a second set of permanent magnets is attached to the base. Both of these components form a thrust bearing where there is no physical contact between the parts. Generated magnetic field forces keep the rotating mass on the air gap, which significantly increases the efficiency of such a system. The entire structure is shielded with sheet metal, divided into several parts. The lower shield (18) is screwed to the underside of the base (2). The upper shield (19) was screwed to the upper plane of the keystone (3). Chamber with the rotating mass was shielded with three metal sheets (20) around the circumference. The electric machine (10) was shielded with one cylinder-shaped cover (21).

After initial designing the shape of the rotating mass, the amount of energy released was calculated. Based on the moment of inertia  $I_y = 40.21 \text{ kg}\cdot\text{m}^2$  of the modelled body read from the Inventor program, the maximum energy from which the energy storage will start to release it was determined. Due to the proposed shape of the rotating mass, its radius was averaged to 0.3 m. Thus, the initial rotational speed of the solid increased to the value  $n_1 = 10,081 \text{ rpm}$ . After substituting these values into the formula (6):

$$E = \frac{I \cdot \omega^2}{2} \quad (6)$$

where:

$I$  – moment of inertia of the modelled body as read out from Inventor,  $\text{kgm}^2$ ,

$\omega$  – maximum angular velocity of the body 12 (Fig. 4),  $\text{rad}\cdot\text{s}^{-1}$ ,

the result was  $E = 22\,409\,168,5 \text{ J} = 6,22 \text{ kWh}$ . Due to the large rotating mass and high rotational speed, the breaking strength of the body was also verified according to the following formula:

$$\sigma_m = \rho \cdot r^2 \cdot \omega^2 \quad (7)$$

where:

$\rho$  – density of material used for rotating body,  $\text{kg/m}^3$ ,

$r$  – averaged radius of a body (due to its shape), m,

$\omega$  – angular velocity of the body,  $\text{rad}\cdot\text{s}^{-1}$ .



The resulting stress  $\sigma_m = 782,5 \text{ MPa}$ , excludes using the cast materials such as cast iron or cast steel due to too low tensile strength. Some structural alloy steels, whose tensile strength exceeds 1,000 MPa, are more suitable for use. However, it must be remembered that such steels will achieve their high strength parameters after heat treatment, and the correct heat treatment of such a large component will be a big technological challenge. Strength requirements are met by titanium alloys whose yield point exceeds 1,000 MPa. Using them, however, will cause a decrease in mass ( $\rho = 4,600 \text{ kg/m}^3$ ), and thus the need to increase the rotational speed of the rotating mass to maintain the assumed amount of energy.

For the modelled body, the energy density stored in the energy storage was checked. For this purpose, the relationship (8), which takes into account the shape of a rotating body, was used. The shape coefficients are given in Table 2.

$$E_{sp} = K \cdot \frac{\sigma_m}{\rho} \quad (8)$$

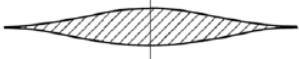
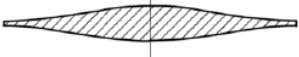



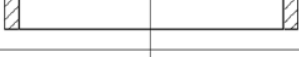

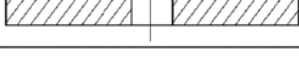
where:

$K$  – shape coefficient of a rotating body,

$\sigma_m$  – tensile stress, Pa,

$\rho$  – density of material used for body,  $\text{kg/m}^3$ .

**Table 2.** K coefficient values for selected shapes of rotating bodies [6, 7]

Laval disk		1.00
Laval disk real		0.70–0.90
Laval-disk-with-rim		0.8–0.95
Conical disk		0.70–0.85
Solid disk		0.606
Thin ring		0.50
Disk with rim and centerhole		0.40–0.50
Thick rim		0.303

In order to calculate the energy density stored in the rotating mass of the shape specified in the model, the coefficient  $K = 0.75$  was assumed on the basis of the first three lines in Table 2. After substituting the values into formula (8), the following expression was obtained:

$$E_{sp} = 20,9 \text{ Wh/kg}$$

The values calculated above were used as input parameters for the selection of the electric machine. For the calculations, it was assumed that the energy storage will be discharged in time  $t_1 = 60$  min from the initial velocity  $\omega_1 = 1055.75 \text{ rad}\cdot\text{s}^{-1}$  to the final velocity  $\omega_2 = 189.6 \text{ rad}\cdot\text{s}^{-1}$ . Thus, the deceleration of the rotating mass was determined according to the following formula:

$$\varepsilon_h = \frac{\omega_1 - \omega_2}{t_1} \quad (9)$$

where:

$\omega_1$  – angular velocity at which energy release begins,  $\text{rad}\cdot\text{s}^{-1}$ ,

$\omega_2$  – angular velocity at which energy release stops,  $\text{rad}\cdot\text{s}^{-1}$ ,

$t$  – time at which energy storage is to be discharged, s.

was the following:

$$\varepsilon_h = \frac{1055,75 - 189,6}{3600} = 0,24 \text{ rad/s}^2.$$

Time of speeding up the rotating mass to nominal angular velocity was assumed to be  $t_2 = 150 \text{ min}$ .

Speeding up of the body to  $\omega_1$  will take place with acceleration  $\varepsilon_r$ :

$$\varepsilon_r = \frac{\omega_1}{t_2} \quad (10)$$

where:

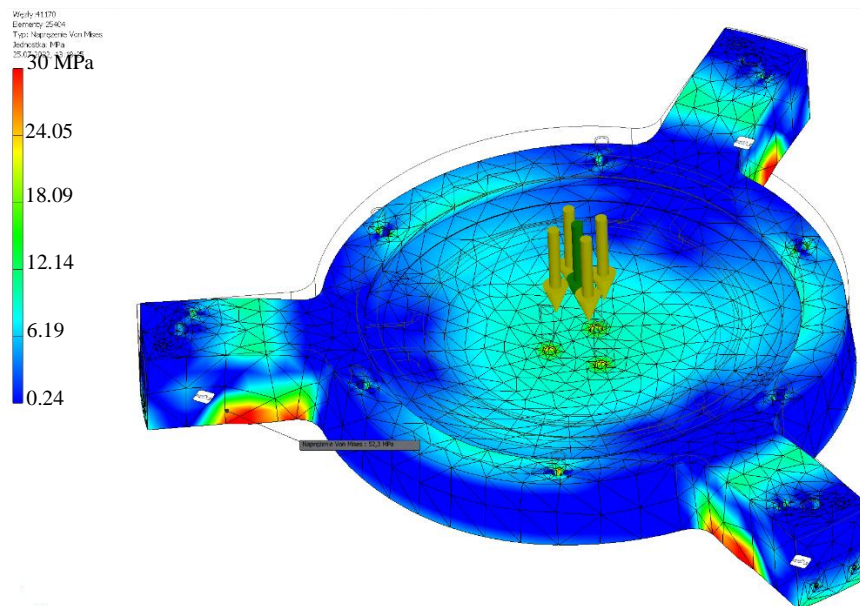
$\omega_1$  – angular velocity at which energy release begins,  $\text{rad}\cdot\text{s}^{-1}$ ,

$t_2$  – time taken for rotor to reach angular velocity  $\omega_1$ , s.

Thus, after substituting to relationship (10), we obtain  $\varepsilon_1 = \frac{1055,75}{9000} = 0,1173 \text{ rad/s}^2$ .

To reach angular velocity  $\omega_1$  of the mass within expected charging time of 150 min, the electric machine should have a torque of at least 4.72 Nm.

Due to the fact that the analyzed energy storage is slow-speed, this will determine its increased dimensions and weight. In terms of strength, base of the frame on which the device will stand was analyzed. The frame is supported at three points. The Finite Element Method was used to analyze the frame in the FEM environment using the Inventor program. The assumed load is 15,000 N.



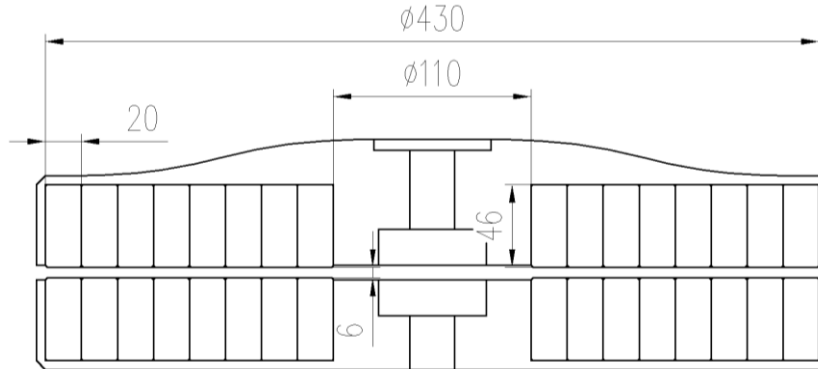
**Fig. 5.** Frame base stress map

The analysis (Fig. 5) shows that the highest stresses occur in the place where the curvature of the frame changes – the transition of the plane into the radius. The role of the radius is to eliminate concentrated stresses on the sharp edge, created by the intersection of the plane on which the feet (11, Fig. 4) are installed to the surface of the cone. The stress value read out in this area is 52.3 MPa. Safety factor for this area is 4, what means that the support should withstand the assumed load.



### 3.3. Calculations of the axial force in the designed magnetic bearing

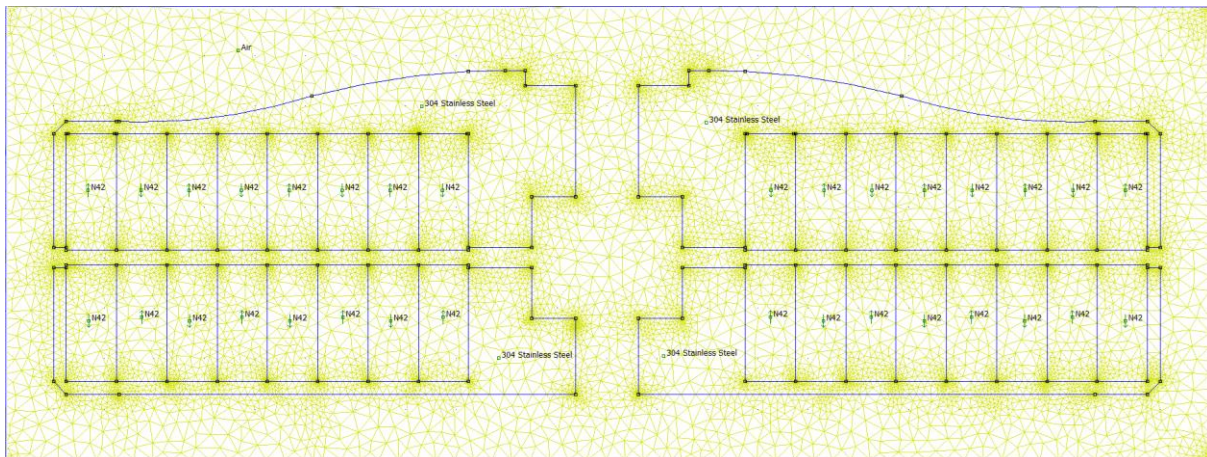
In order to reduce the work resistance during spinning, a magnetic bearing made of permanent magnets was used. A cross-section through a magnetic bearing acting as a thrust bearing, in which the system of permanent magnets is shown in Fig. 6. The drawing of the bearing node was used to calculate the support force generated by the set of permanent magnets of the bearing.



**Fig. 6.** Dimensions of the magnetic bearing cross-section

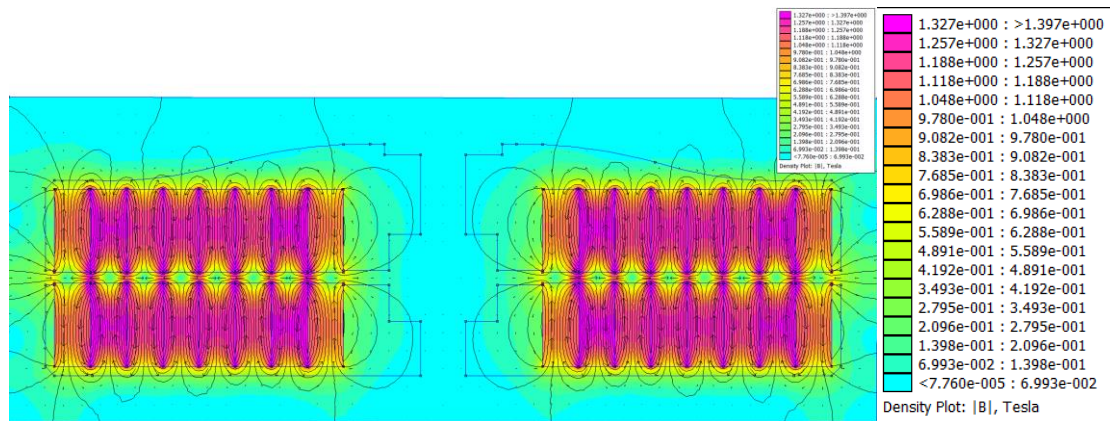
The cross-section in Fig. 6 was used to build the geometrical form of the numerical model of the magnetic bearing, created in the FEM 4.2 program. This program enables calculations of magnetic field strengths and interaction forces for 2D models of a given thickness.

Figure 7 shows a digital computational model with the directions of magnetic poles for each permanent magnet and the finite element meshing. The magnets in the disc are arranged alternately with magnetic pairs. The magnets are made of Neodymium N42. The alternating arrangement of the pairs will increase the force of interaction between the bearing disks several times.



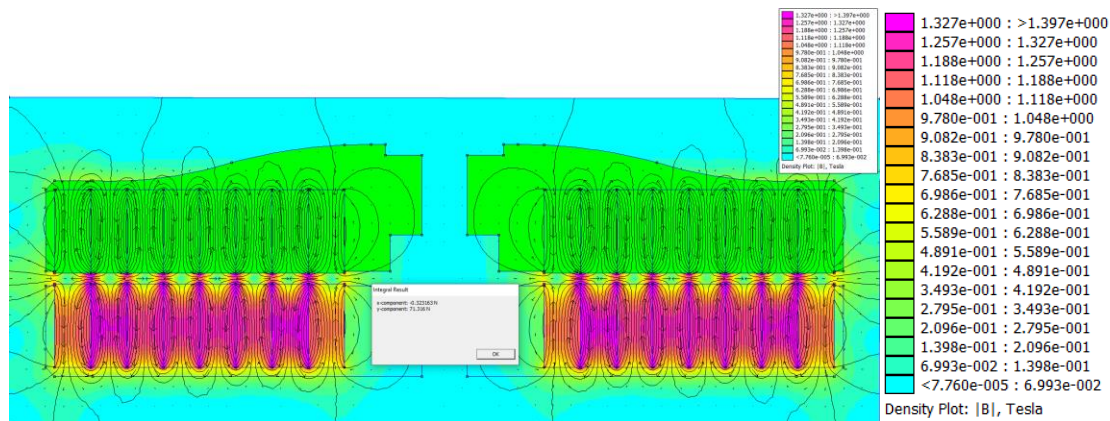
**Fig. 7.** Computational model with the direction of magnetic poles developed in FEM 4.2

The results of numerical calculations in a map form with the magnetic field strength and lines of force are shown in Figure 8.



**Fig. 8.** Distribution of magnetic field lines against the background of the magnetic field strength map in a magnetic bearing

Figure 9 shows simulation of the force acting on the upper disc (marked in green). Calculated interaction force of 71.3 N corresponds to a 1 mm layer of magnets.



**Fig. 9.** Interaction force between the magnetic bearing discs for a 1 mm magnetic layer

Calculated force for a 1 mm layer was multiplied by the thickness of applied permanent magnets. The approximate force in the magnetic bearing will be 30.2 kN. This is the value of magnetic field strength for a 6 mm gap. This force is sufficient for the designed rotor-loaded bearing. For a 10 kN load, the gap between the discs will increase to approx. 10 mm.

#### 4. Conclusions

The concept of low-speed kinetic energy storage - LSFESS fills a significant gap in the field of energy storage dedicated to individual households. In the case of prosumer applications, high-speed energy storages used in industrial conditions have significant disadvantages regarding very high operating costs and complicated maintenance [8, 9].

The overall dimensions of the LSFESS, developed in accordance with the presented concept, allow it to be moved through standard passages and crossings and placed in spaces that do not require special preparation. Problematic in this case is the total weight of the device, which exceeds 1,000 kg. In LSFESS there is also a much more easy-to-use and compact control and supervision system for the device operation. The device is assumed to be maintenance-free on the part of the potential user. However, it should be subject to an annual technical inspection by a specialized service.

The energy density accumulated in the proposed solution is nearly 21 Wh/kg.

In the case of slow-speed energy storage, where the rotors are most often made of steel [4], for rotating steel masses, a maximum 40 Wh/kg can be achieved. It can therefore be concluded that more detailed research work on the shape and mass of the rotor is required to achieve a higher energy density. However, for the assumed parameters of the energy storage, this may be difficult to achieve.

## References

- [1] Volvo Cars. Volvo Cars Tests of Flywheel Technology Confirm Fuel Savings of Up to 25 Percent. 2013. <https://www.media.volvocars.com/global/en-gb/media/pressreleases/48800> [accessed: 28.09.2022]
- [2] <https://www.car-engineer.com/flywheel-technology-tested-on-volvo-s60-shows-important-fuel-savings/> [accessed: 28.09.2022]
- [3] <https://www.railwayage.com/passenger/rapid-transit/la-metro-vycon-wess-system-saving-energy/> (dostęp 21 października 2021).
- [4] <https://mttechnology.pl/> [accessed: 28.09.2022]
- [5] Olabi A., Wilberforce T., Abdelkareem M., Ramadan M. Critical Review of Flywheel Energy Storage System. *Energies* 2021, 14, 2159, str. 29-33. DOI: 10.3390/en-14082159.
- [6] Östergård R. Flywheel energy storage a conceptual study. Uppsala Universitet 2011.
- [7] Ertz G., Twiefel J., Krack M. Feasibility Study for Small Scaling Flywheel-Energy-Storage Systems in Energy Harvesting Systems. *Energy Harvesting and Systems* 2014 1(3-4): ss. 233–241. DOI: 10.1515/ehs-2013-0010
- [8] Hedlund M., Lundin J., Santiago J., Abrahamsson J., Bernhoff H. Flywheel Energy Storage for Automotive Applications. *Energies* 2015, 8, str. 10636-10663. DOI: 10.3390/en-81010636
- [9] Khandoker H., Hawkins S. C., Ibrahim R., Huynh C. P., Deng F., Tensile strength of spinnable multiwall carbon nanotubes. *Science Direct. Engineering Procedia* 10 (2011) 2572-2578 DOI: 10.1016/j.proeng.2011.04.424

